Dynamic Analysis of SSI Systems via a Coupled Finite-element/Scaled Boundary Finite-element Model

***D. Chen[1], C. Birk[2], and S. Dai[3]**

[1]College of Civil Engineering and Architecture, China Three Gorges University, Yichang 443002, China
[2]School of Civil and Environmental Engineering, University of New South Wales, Sydney, NSW 2052, Australia
[3]College of Mechanics and Materials, Hohai University, Nanjing 210098, China

*Corresponding author: chdenghong@gmail.com

Abstract

A coupled model based on finite element method (FEM) and scaled boundary finite element method (SBFEM) for transient dynamic response of large-scale SSI systems is presented. The well-established FEM is used for modeling the near-field bounded domains. A local high-order transmitting boundary, which is based on SBFEM and the improved continued fraction solution for the dynamic stiffness matrix, is used for modeling the dynamic response of the far-field unbounded domains. The bounded and unbounded formulations are coupled via the interaction force vector at the interface. The standard equations of the coupled model in the time domain are obtained by combining the dynamic equations of bounded and unbounded domains, which can be solved by a direct time-domain integration method. The stability of the coupled system depends on the general eigenproblem of the coefficient matrices. Possible spurious modes can be eliminated using the spectral shifting technique. The validity of the coupled model is shown by means of two numerical examples.

Keywords: Dynamic soil-structure interaction, Coupled FEM-SBFEM model, High-order transmitting boundary, Spectral shifting technique.

1 Introduction

Dynamic soil-structure interaction plays an important role in the design and safety assessment of structures, especially for large-scale structures, such as concrete dams, nuclear power plants, bridges etc. A rational and commonly used approach for modeling the whole system is to divide it into two parts. The first part is the near-field bounded domain, which contains the structure and a part of the adjacent soil and can be efficiently modeled by the finite element method. The second part is the far-field unbounded domain, which includes the rest of the infinite foundation. The major challenge is the accurate description of radiation damping at infinity. Here, the well-established finite element method cannot be used straightforwardly, since outgoing waves are reflected at the artificial boundaries of the finite element mesh.

Over the past few decades, many numerical methods have been developed to model the wave propagation in unbounded domains. Generally, they can be classified into two groups, global and local procedures. The global procedures include the boundary element method (Beskos, 1987; Beskos, 1997), the thin layer method (Kausel, 1986; Kausel, 1994), exact non-reflecting boundaries (Keller and Givoli, 1989) and the scaled boundary finite element method (Wolf and Song, 1996). The local procedures include the viscous boundary (Lysmer and Kuhlemeyer, 1969), the viscous-spring boundary (Deeks and Randolph, 1994; Liu *et al.*, 2006), the artificial transmitting boundary (Liao *et al.*, 1984), infinite elements (Zhao, 2009) and high-order absorbing boundary conditions (Engquist and Majda, 1977; Higdon, 1986; Bayliss and Turkel, 1980). The advantages, disadvantages and some progresses of these methods have been summarized in the review literatures (Tsynkov, 1998; Givoli, 2004; Lou *et al.*, 2011) and are not repeated here.

The scaled boundary finite element method, developed by Wolf and Song in 1990s, is a semi-analytical technique which excels in modelling wave propagation in unbounded and bounded domains. This method has the following distinguished features. First of all, the radiation condition for unbounded domain is satisfied rigorously without requiring a fundamental solution. Secondly, only the boundary of the domain is discretized as in the boundary element method, and the spatial dimension is reduced by one. Moreover, this method can be coupled seamlessly with the standard finite element method. Utilizing the advantages of the scaled boundary finite element method, many scholars have adopted it to study dynamic soil-structure interaction problems.

Zhang *et al.* (1999) applied a piecewise linear approximation of the acceleration unit-impulse response matrix of the unbounded domain within one time step and simplified the solution of the time-consuming convolution integrals. Yan *et al.* (2004) coupled the finite element method and the scaled boundary finite element method for 3D dynamic analysis of soil-structure interaction in the time domain. Linear system theory was employed to improve the efficiency for solving the acceleration unit-impulse response matrix of the unbounded domain. Radmanovic and Katz (2012) made two improvements to the original method. Genes (2012) reported a coupled model for dynamic analysis of 2D large-scale SSI systems based on finite element method, boundary element method and scaled boundary finite element method, and presented a parallel computation algorithm for the coupled model. Schauer *et al.* (2011, 2012) introduced a parallel algorithm for a coupled finite element - scaled boundary finite element approach to study soil-structure-interaction problems. Due to high computational cost resulting from the application of SBFEM to large-scale problems, parallel computing based on PC clusters was employed to improve the computational efficiency.

The original solution procedure, which is based on the solution of the acceleration unit-impulse response matrix of the unbounded domain, was commonly used in the above references. It is global in time and space, and thus computationally expensive. Alternative procedures, which aim at avoiding the convolution integral altogether by developing the scaled boundary finite element method directly in the time domain, have been proposed recently. Song and Bazyar (2008) proposed a Padé approximation for the dynamic stiffness matrix of an unbounded medium in the frequency domain, which has a large range and high rate of convergence. Bazyar and Song (2008) then developed a high-order local transmitting boundary based on a continued-fraction solution of the dynamic stiffness matrix. But the method may fail for systems with a larger number of degrees of freedom and for approximations of higher order. Birk *et al.* (2012) presented an improved continued-fraction solution for the dynamic stiffness matrix of an unbounded domain, which is numerically more robust and suitable for large-scale systems and arbitrarily high orders of expansion.

This paper aims to develop a new coupled method that combines the bounded and unbounded domains in the time domain. Here, the bounded domain is modeled by the well-established finite element method. The unbounded domain is represented by the high-order transmitting boundary, which is based on the improved continued fraction solution for the dynamic stiffness matrix.

The rest of the paper is outlined as follows. Section 2 describes some basic equations about the scaled boundary finite element method. Section 3 presents a new coupled method of bounded and unbounded domains. Section 4 demonstrates the application of the proposed coupled method to two numerical examples. Section 5 summarizes some major conclusions from this contribution.

2 Summary of the scaled boundary finite element method

The scaled boundary finite element method is introduced in detail by Wolf and Song (1996). For completeness, only some main equations are summarized in this part.

The scaled boundary finite element method is described in a local coordinate system, η, ζ on the boundary and the radial coordinate ξ. SBFEM defines the whole domain by scaling a boundary S relative to a scaling center O. The normalized radial coordinate ξ is a scaling factor, defined as 1 at the boundary S and 0 at the scaling center O. For a bounded domain, $0 \le \xi \le 1$; whereas, for an unbounded domain, $1 \le \xi < +\infty$.

The displacements at a point (ξ, η, ζ) are interpolated as

$$\{u(\xi,\eta,\zeta)\} = [N(\eta,\zeta)]\{u(\xi)\} = [N_1(\eta,\zeta)[I],\ N_2(\eta,\zeta)[I], \ldots]\{u(\xi)\} \tag{1}$$

where $[N(\eta,\zeta)]$ are the shape functions in the circumferential directions. $\{u(\xi)\}$ are the displacements along the radial lines and are analytical with respect to ξ only.

The strains are derived as

$$\{\varepsilon(\xi,\eta,\zeta)\} = [B^1(\eta,\zeta)]\{u(\xi)\}_{,\xi} + \frac{1}{\xi}[B^2(\eta,\zeta)]\{u(\xi)\} \tag{2}$$

where $[B^1(\eta,\zeta)]$ and $[B^2(\eta,\zeta)]$ represent the strain-nodal displacement relationship.

The stresses and strains are related by the elastic matrix $[D]$

$$\{\sigma(\xi,\eta,\zeta)\} = [D]\{\varepsilon(\xi,\eta,\zeta)\} \tag{3}$$

After expressing the governing differential equations in the scaled boundary coordinates, Galerkin's weighted residual method or the virtual work formulation (Deeks and Wolf, 2002) is applied in the circumferential directions. In the frequency domain, the scaled boundary finite element equation in displacement is expressed as

$$[E^0]\xi^2\{u(\xi)\}_{,\xi\xi} + \left((s-1)[E^0] - [E^1] + [E^1]^T\right)\xi\{u(\xi)\}_{,\xi} + \left((s-2)[E^1]^T - [E^2]\right)\{u(\xi)\} + \omega^2[M^0]\xi^2\{u(\xi)\} = 0 \tag{4}$$

where s (=2 or 3) denotes the spatial dimension of the domain, and ω is the excitation frequency. The coefficient matrices $[E^0]$, $[E^1]$, $[E^2]$, and $[M^0]$ are obtained by assembling the element coefficient matrices calculated on the boundary. The coefficient matrices are written for three-dimensional elastodynamics as

$$[E^0] = \int_{-1}^{+1}\int_{-1}^{+1}[B^1(\eta,\zeta)]^T[D][B^1(\eta,\zeta)]\left|J(\eta,\zeta)\right|d\eta d\zeta \tag{5a}$$

$$[E^1] = \int_{-1}^{+1}\int_{-1}^{+1}[B^2(\eta,\zeta)]^T[D][B^1(\eta,\zeta)]\left|J(\eta,\zeta)\right|d\eta d\zeta \tag{5b}$$

$$[E^2] = \int_{-1}^{+1}\int_{-1}^{+1}[B^2(\eta,\zeta)]^T[D][B^2(\eta,\zeta)]\left|J(\eta,\zeta)\right|d\eta d\zeta \tag{5c}$$

$$[M^0] = \int_{-1}^{+1}\int_{-1}^{+1}[N(\eta,\zeta)]^T\rho[N(\eta,\zeta)]\left|J(\eta,\zeta)\right|d\eta d\zeta \tag{5d}$$

3 Coupled method of bounded and unbounded domains

3.1 Bounded domain

The equation of motion of the bounded domain in the time domain can be expressed as

$$\begin{bmatrix}[M_{ss}] & [M_{sb}]\\ [M_{bs}] & [M_{bb}]\end{bmatrix}\begin{Bmatrix}\{\ddot{u}_s\}\\ \{\ddot{u}_b\}\end{Bmatrix} + \begin{bmatrix}[K_{ss}] & [K_{sb}]\\ [K_{bs}] & [K_{bb}]\end{bmatrix}\begin{Bmatrix}\{u_s\}\\ \{u_b\}\end{Bmatrix} = \begin{Bmatrix}\{P_s\}\\ \{P_b\}\end{Bmatrix} - \begin{Bmatrix}\{0\}\\ \{R_b\}\end{Bmatrix} \tag{6}$$

where $[M]$ and $[K]$ are the mass and stiffness matrices of the bounded domain, $\{\ddot{u}\}$, $\{\dot{u}\}$, $\{u\}$ are the acceleration, velocity and displacement vectors, $\{P\}$ is an external force vector acting directly on the bounded domain, while $\{R\}$ is an interaction force vector acting at the soil-structure interface. Subscript s describes the nodes belonging only to the bounded domain, b denotes the notes at the boundary belonging to both, the bounded and unbounded domains. Here, the stiffness matrix $[K]$ and mass matrix $[M]$ are assembled by the finite element method (Zienkiewicz *et al.*, 2005).

3.2 Unbounded domain

For an unbounded domain, the scaled boundary finite element equation in dynamic stiffness is expressed as

$$\left([S^{\infty}(\omega)]+[E^{1}]\right)[E^{0}]^{-1}\left([S^{\infty}(\omega)]+[E^{1}]^{T}\right)-(s-2)[S^{\infty}(\omega)]-\omega[S^{\infty}(\omega)]_{,\omega}-[E^{2}]+\omega^{2}[M^{0}]=0 \quad (6)$$

The continued fraction solution for $[S^{\infty}(\omega)]$ at the high-frequency limit ($\omega\to\infty$) is expressed as

$$[S^{\infty}(\omega)]=[K_{\infty}]+i\omega[C_{\infty}]-[X^{(1)}][Y^{(1)}(\omega)]^{-1}[X^{(1)}]^{T} \quad (7a)$$

$$[Y^{(i)}(\omega)]=[Y_0^{(i)}]+i\omega[Y_1^{(i)}]-[X^{(i+1)}][Y^{(i+1)}(\omega)]^{-1}[X^{(i+1)}]^{T} \quad (i=1,2\cdots,M_{cf}) \quad (7b)$$

where $[K_{\infty}]$, $[C_{\infty}]$, $[Y_0^{(i)}]$ and $[Y_1^{(i)}]$ are coefficient matrices to be determined recursively in the solution procedure. M_{cf} is the order of the continued fraction expansion. The solution of these coefficient matrices is described in detail in the work by Birk *et al.* (2012) and not repeated here. The additional factor matrices $[X^{(1)}]$ and $[X^{(i+1)}]$ are introduced to improve the numerical stability of the solution. In the original method (Bazyar and Song, 2008), the coefficient matrix $[X^{(1)}]$ is taken as a unit matrix $[I]$. But it may cause numerical difficulty or even erroneous results, especially for the systems with many degrees of freedom and high orders of continued fraction expansion. So an improved continued fraction method (Birk *et al.*, 2012) is developed to overcome the numerical problem. Compared to the original approach, it leads to numerically more robust formulations and is therefore suitable for large-scale systems and arbitrarily high orders of expansion. The **LDL**^{T} decomposition (Golub and Van Loan, 1996) is employed to obtain $[X^{(i)}]$.

Using the improved continued fraction solution of the dynamic stiffness and introducing auxiliary variables, the force-displacement relationship with $\xi=1$ on the boundary is expressed in the time domain as

$$[K_u]\{z(t)\}+[C_u]\{\dot{z}(t)\}=\{f(t)\} \quad (8)$$

with

$$[K_u]=\begin{bmatrix} [K_{\infty}] & -[X^{(1)}] & 0 & \cdots & 0 & 0 \\ -[X^{(1)}]^{T} & [Y_0^{(1)}] & -[X^{(2)}] & \cdots & 0 & 0 \\ 0 & -[X^{(2)}]^{T} & [Y_0^{(2)}] & \cdots & 0 & 0 \\ \vdots & \vdots & \vdots & \ddots & -[X^{(M_{cf}-1)}] & 0 \\ 0 & 0 & 0 & -[X^{(M_{cf}-1)}]^{T} & [Y_0^{(M_{cf}-1)}] & -[X^{(M_{cf})}] \\ 0 & 0 & 0 & 0 & -[X^{(M_{cf})}]^{T} & [Y_0^{(M_{cf})}] \end{bmatrix} \quad (9a)$$

$$[C_u]=\begin{bmatrix}[C_\infty] & & & & & \\ & [Y_1^{(1)}] & & & & \\ & & [Y_1^{(2)}] & & & \\ & & & \ddots & & \\ & & & & [Y_1^{(M_{cf}-1)}] & \\ & & & & & [Y_1^{(M_{cf})}]\end{bmatrix} \tag{9b}$$

$$\{z(t)\}=\begin{Bmatrix}\{u_b\}\\ \{u^{(1)}\}\\ \{u^{(2)}\}\\ \vdots\\ \{u^{(M_{cf}-1)}\}\\ \{u^{(M_{cf})}\}\end{Bmatrix},\quad \{f(t)\}=\begin{Bmatrix}\{R_b\}\\ \{0\}\\ \{0\}\\ \vdots\\ \{0\}\\ \{0\}\end{Bmatrix} \tag{9c}$$

where the vector $\{z\}$ consists of the displacement vector $\{u_b\}$ and the auxiliary variables $\{u^{(i)}\}$ on the boundary. The vector $\{f\}$ contains the coupling forces $\{R_b\}$ on the boundary.

3.3 Coupled method of bounded and unbounded domains

The bounded and unbounded domain formulations are coupled via the interaction force vector $\{R_b\}$. For a linear system, the coupled equations of the bounded and unbounded domain in the time domain are obtained by combining Equation (6) and (8). It yields

$$[K_c]\{d_c\}+[C_c]\{\dot{d}_c\}+[M_c]\{\ddot{d}_c\}=\{f_c\} \tag{10}$$

with

$$[K_c]=\begin{bmatrix}[K_{ss}] & [K_{sb}] & & & & & & \\ [K_{bs}] & [K_{bb}]+[K_\infty] & -[X^{(1)}] & & & & & \\ & -[X^{(1)}]^T & [Y_0^{(1)}] & -[X^{(2)}] & & & & \\ & & -[X^{(2)}]^T & [Y_0^{(2)}] & & & & \\ & & & & \ddots & -[X^{(M_{cf}-1)}] & & \\ & & & & -[X^{(M_{cf}-1)}]^T & [Y_0^{(M_{cf}-1)}] & -[X^{(M_{cf})}] & \\ & & & & & -[X^{(M_{cf})}]^T & [Y_0^{(M_{cf})}] & \end{bmatrix} \tag{11a}$$

$$[C_c]=\begin{bmatrix}[0] & [0] & & & & & & \\ [0] & [C_\infty] & & & & & & \\ & & [Y_1^{(1)}] & & & & & \\ & & & [Y_1^{(2)}] & & & & \\ & & & & \ddots & & & \\ & & & & & [Y_1^{(M_{cf}-1)}] & & \\ & & & & & & [Y_1^{(M_{cf})}] & \end{bmatrix} \tag{11b}$$

$$[M_c]=\begin{bmatrix} [M_{ss}] & [M_{sb}] & & & & & \\ [M_{bs}] & [M_{bb}] & & & & & \\ & & [0] & & & & \\ & & & [0] & & & \\ & & & & \ddots & & \\ & & & & & [0] & \\ & & & & & & [0] \end{bmatrix} \tag{11c}$$

$$\{d_c\}=\left(\{u_s\} \quad \{u_b\} \quad \{u^{(1)}\} \quad \{u^{(2)}\} \quad \cdots \quad \{u^{(M_{cf}-1)}\} \quad \{u^{(M_{cf})}\}\right)^T \tag{11d}$$

$$\{f_c\}=\left(\{P_s(t)\} \quad \{P_b(t)\} \quad \{0\} \quad \{0\} \quad \cdots \quad \{0\} \quad \{0\}\right)^T \tag{11e}$$

Equation (10) is a standard equation of motion with sparse symmetric matrices in the time domain. It can be converted to be a system of first-order ordinary differential equations with high-order stiffness and damping matrices.

$$[K_{global}]\{z_{global}\}+[C_{global}]\{\dot{z}_{global}\}=\{P_{global}\} \tag{12}$$

Equation (12) can be easily solved by a direct time-domain integration method (Adhikari and Wagner, 2004). It should be noted that the stability of Equation (12) depends on the general eigenproblem for the coefficient matrices $[K_{global}]$ and $[C_{global}]$. If some positive real parts of the general eigenvalues are observed, the system will be instable. Therefore, it is very important to eliminate these spurious modes using the spectral shifting technique (Trinks, 2004).

4 Numerical examples

4.1 Example 1: Dynamic response of an elastic block on a homogeneous half-space soil

The dynamic response of an elastic block on a homogenous half-space soil as shown in Figure 1 is studied. The soil's properties are: shear modulus $G_1=G$, Poisson's ratio $\nu_1=0.25$, mass density $\rho_1=\rho$. The properties of the elastic block are: shear modulus $G_2=G$, Poisson's ratio $\nu_2=0.25$, mass density $\rho_2=\rho$. Plain strain state is considered. A uniformly distributed pressure $P(t)$ with an amplitude P and a duration $3b/c_s$ as shown in Figure 2 is applied on the top surface of the elastic block. This series of two triangular force pulses of different duration represents a combination of high and low frequency loading. The fixed time step $\Delta t=0.02b/c_s$ is selected.

In the coupled method, the block and soil are discretized with 288 four-node finite elements and 325 nodes as shown in Figure 3. The unbounded domain is modelled using the high-order transmitting boundary. It is discretized with 24 two-node line elements and 25 nodes. The scaling center of the unbounded domain is chosen at point O as shown in Figure 1. The dynamic analysis is performed using authors' Matlab code.

To evaluate the accuracy of the proposed coupled method, an extended mesh with a rectangle area $21b\times20b$ to the right of plain of symmetry is analysed using the finite element method. Only half of the symmetric system is discretized with 6768 eight-node elements of size $0.25b\times0.25b$, yielding 20657 nodes. A fixed boundary condition is adopted in the reference finite element model. The implicit analysis is carried out using the commercial finite element software ABAQUS/Standard (ABAQUS, 2010).

The vertical displacement responses at points A, O (see Figure 1) are plotted in Figure 4. The

results are non-dimensionalised with P/G. In case of the order M_{cf}=9, the results agree very well with the reference solution for time up to $\bar{t} = 10$. After that, slight deviations can be observed. By increasing the order to M_{cf}=15, the agreement between the results of the coupled method and those of the extended mesh is excellent.

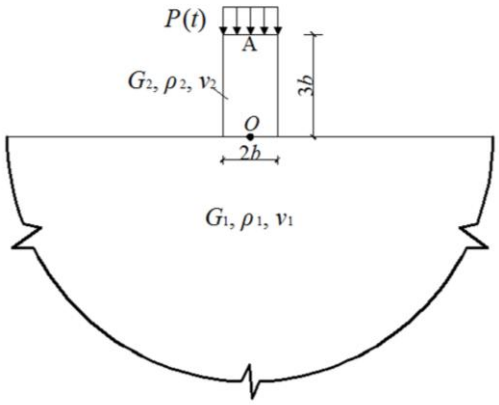

Figure 1. Elastic block and half-space under strip loading

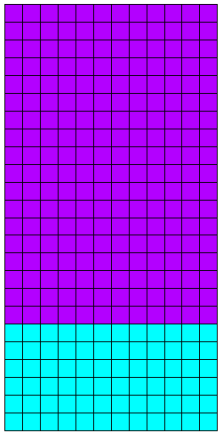

Figure 3. FE mesh of the coupled system

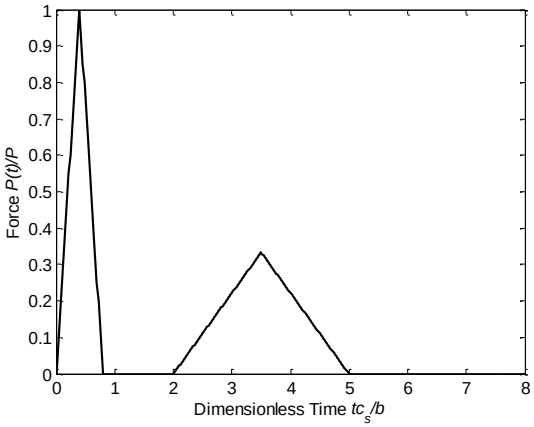

(a) Time domain

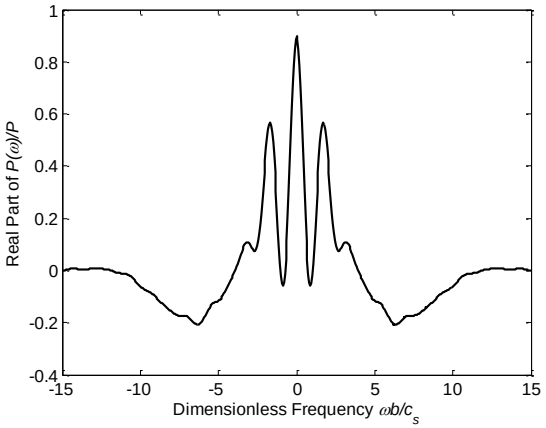

(b) Frequency domain

Figure 2. Series of two triangular force pulses

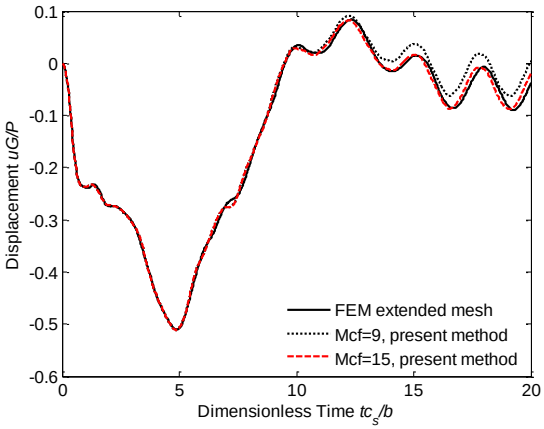

(a) Point A

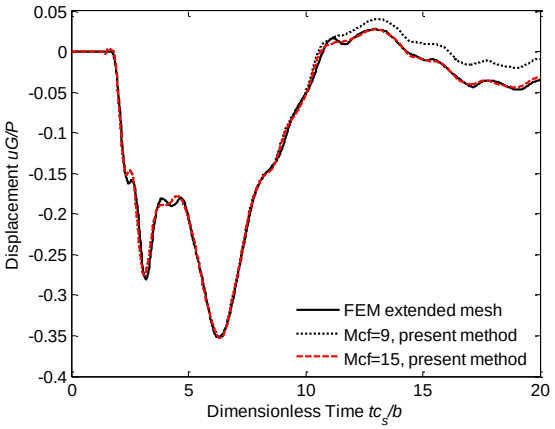

(b) Point O

Figure 4. Dimensionless vertical displacements

4.2 Example 2: Seismic response of a gravity dam-foundation system

As an application example, the seismic response of a concrete gravity dam as shown in Figure 5 is investigated. The concrete gravity dam of 89 m high is constructed on a homogenous semi-infinite rock foundation, which is extended to infinity. The dam's properties are: modulus of elasticity E_c=25.44 GPa, Poisson's ratio ν_c=0.20 and unit weight γ_c=26.0 kN/m^3. The properties of the semi-infinite rock foundation are exactly the same as those of the concrete. Plain strain state is considered. The design peak ground accelerations are 0.399g in the horizontal direction and 0.266g in the vertical direction, where g is the gravitational acceleration. The horizontal and vertical (2/3 horizontal) components of the 1967 KOYNA earthquake records (see Figure 6) are applied to the nodes of the dam body. The performance of the dam for only empty reservoir condition is studied.

In the coupled method, the system is discretized with 288 four-node finite elements and 325 nodes as shown in Figure 7. The semi-infinite foundation is discretized with 24 two-node line elements and 25 nodes. The scaling center of the semi-infinite foundation is located at the center of the dam-foundation interface. The fixed time step Δt=0.02s is selected.

In order to obtain another reference solution that can be compared with the proposed solution, the range of the dam foundation is extended to 2×10^4 m toward the upstream, downstream directions and 2×10^4 m in the vertical direction. The dam and foundation are discretized with 186520 four-node elements and 187467 nodes.

Time histories of the horizontal and vertical displacements at dam crest are plotted in Figure 8. Clearly, the numerical results obtained from the coupled method (M_{cf}=12) agree well with those obtained from the extended mesh. For the solutions of the extended mesh and the coupled method, the maximum horizontal displacements at dam crest are 3.44 cm and 3.33 cm, respectively. The maximum vertical displacements at dam crest are 1.09 cm and 1.05 cm, respectively. The relative errors of the horizontal and vertical displacements are 3.39% and 3.73%, respectively, which are both less than 5% and acceptable from an engineering point of view.

To evaluate the efficiency of the coupled method, the computer times spent on the above analyses are recorded on a computer with Intel(R) Pentium(R) CPU G840 @ 2.80GHz and 4GB RAM. The extended meh and present approach in Example 1 take 37min41s and 7min57s, respectively. The computer times for the extended mesh and present approach of Example 2 are 2h13min46s and 7min2s, respectively. Obviously, the present approach is more efficient.

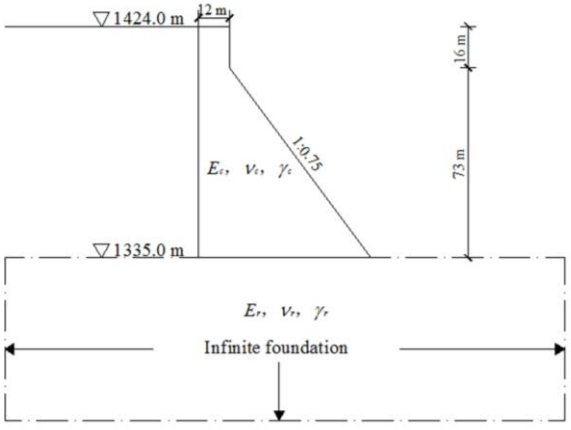

Figure 5. The gravity dam in section

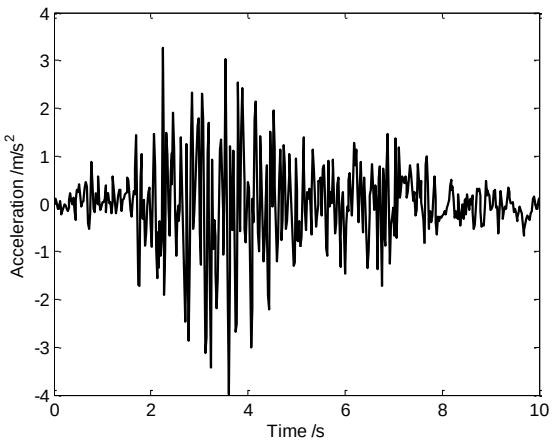

Figure 6. The input earthquake acceleration

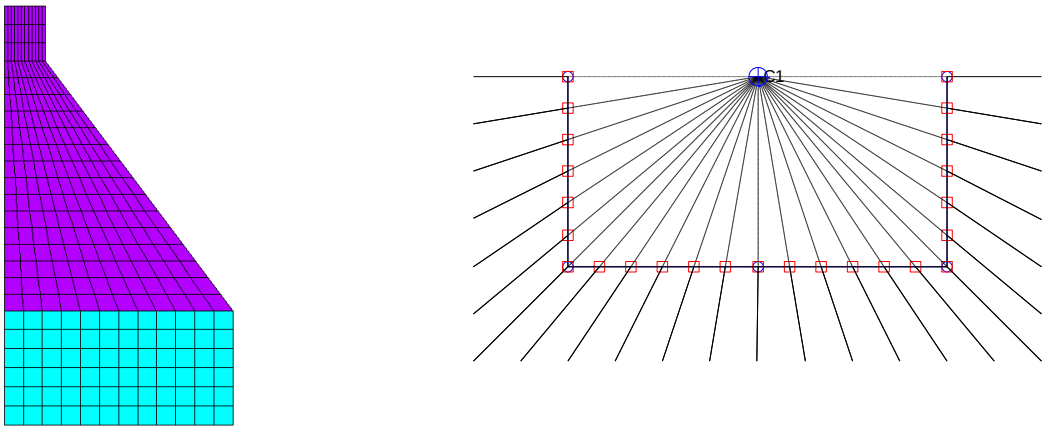

(a) FE mesh of the system (b) SBFE mesh of the unbounded domain

Figure 7. Mesh of the gravity dam-foundation system

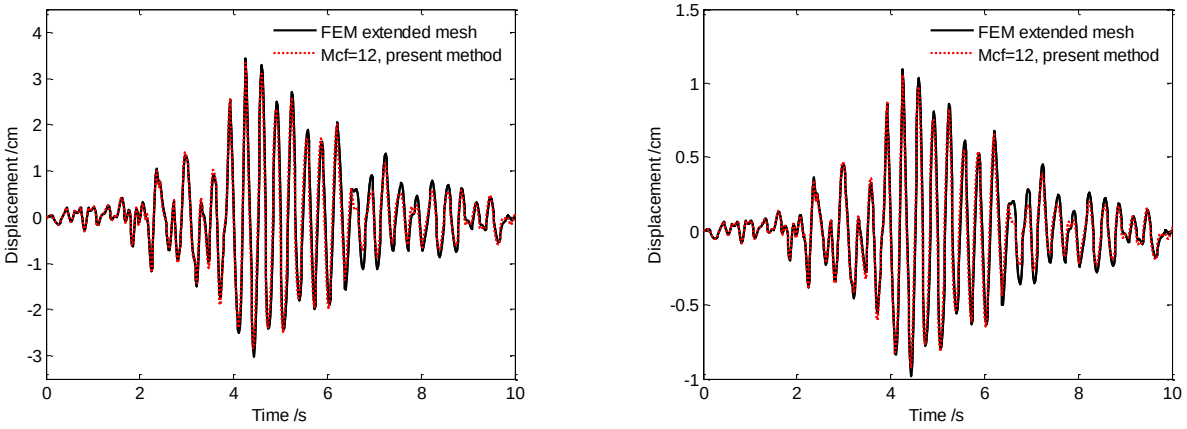

(a) Horizontal (b) Vertical

Figure 8. Time histories of displacements at dam crest

5 Conclusions

A novel coupled method of bounded and unbounded domains is presented. The near-field bounded domain is modeled by the well-established finite elements. The far-field unbounded domain is represented by the high-order transmitting boundary, which is based on the improved continued fraction solution for the dynamic stiffness matrix of the unbounded domain. The coupled standard equation of motion of a linear system in the time domain is obtained by combining the dynamic equations of bounded and unbounded domains, which can be solved by a direct time-domain integration method. The results of two numerical examples demonstrate that the coupled method is more accurate and efficient in the time domain. The approach presented in this paper can easily be extended to three-dimensional problems, further study is ongoing.

Acknowledgements

This work was supported by the Science Foundation of China Three Gorges University (Grant No. KJ2013B003). This support is gratefully acknowledged.

References

Beskos, D. E. (1987), Boundary element methods in dynamic analysis. *Applied Mechanics Reviews*, 40, pp. 1–23.

Beskos, D. E. (1997), Boundary element methods in dynamic analysis: Part II (1986-1996). *Applied Mechanics Reviews*, 50, pp. 149–197.

Kausel, E. (1986), Wave propagation in anisotropic layered media. *International Journal for Numerical Methods in Engineering*, 23, pp. 1567–1578.
Kausel, E. (1994), Thin-layer method: formulation in the time domain. *International Journal for Numerical Methods in Engineering*, 37, pp. 927–941.
Keller, J. B and Givoli, D. (1989), Exact non-reflecting boundary conditions. *Journal of Computational Physics*, 82, pp. 172–192.
Wolf, J. P. and Song, Ch. (1996), *Finite-element modeling of unbounded media*. Wiley: New York.
Lysmer, J. and Kuhlemeyer, R. L. (1969), Finite dynamic model for infinite media. *Journal of Engineering Mechanics, ASCE*, 95, pp. 759–877.
Deeks, A. J. and Randolph, M. F. (1994), Axisymmetric time-domain transmitting boundaries. *Journal of Engineering Mechanics, ASCE*, 120, pp. 25–42.
Liu, J. B., Du, Y. X. and Du, X. L. (2006), 3D viscous-spring artificial boundary in time domain. *Earthquake Engineering and Engineering Vibration*, 5, pp. 93–102.
Liao, Z. P., Wong, H. L. and Yang, B. (1984), A transmitting boundary for transient wave analyses. *Scientia Sincia Methematica*, 27, pp. 1063–1076.
Zhao, C. B. (2009), *Dynamic and transient infinite elements: theory and geophysical, geotechnical and geoenvironmental applications*. Springer: Berlin.
Engquist, B. and Majda, A. (1977), Absorbing boundary conditions for the numerical simulation of waves. *Mathematics of Computation*, 31, pp. 629–651.
Higdon, R. L. (1986), Absorbing boundary conditions for difference approximations to multi-dimensional wave equation. *Mathematics and Computation*, 47, pp. 437–459.
Bayliss, A. and Turkel, E. (1980), Radiation boundary conditions for wave-like equations. *Communications on Pure and Applied Mathematics*, 33, pp. 707–725.
Tsynkov, S. V. (1998), Numerical solution of problems on unbounded domains. A review. *Applied Numerical Mathematics*, 27, pp. 465–532.
Givoli, D. (2004), High-order local non-reflecting boundary conditions: a review. *Wave Motion*, 39, pp. 319–326.
Lou, M. L., Wang, H. F., Chen, X. and Zhai, Y. M. (2011), Structure-soil-structure interaction: Literature review. *Soil Dynamics and Earthquake Engineering*, 31, pp. 1724–1731.
Zhang, X., Wegner, J. L. and Haddow, J. B. (1999), Three-dimensional dynamic soil-structure interaction analysis in the time domain. *Earthquake Engineering and Structural Dynamics*, 28, pp. 1501–1524.
Yan, J. Y., Zhang, C. H. and Jin, F. (2004), A coupling procedure of FE and SBFE for soil-structure interaction in the time domain. *International Journal for Numerical Methods in Engineering*, 59, pp. 1453–1471.
Radmanovic, B. and Katz, C. (2012), Dynamic soil-structure interaction using an efficient scaled boundary finite element method in time domain with examples. *SECED Newsletter*, 23(3), pp. 3–14.
Genes, M. C. (2012), Dynamic analysis of large-scale SSI systems for layered unbounded media via a parallelized coupled finite element/boundary element/scaled boundary finite element model. *Engineering Analysis with Boundary Elements*, 36, pp. 845–857.
Schauer, M., Langer, S., Roman, J. E. and Quintana-Ort ́ı E. S. (2011), Large scale simulation of wave propagation in soils interacting with structures using FEM and SBFEM. *Journal of Computational Acoustics*, 19, pp. 75–93.
Schauer, M., Roman, J. E., Quintana-Ort ́ı E. S. and Langer, S. (2012), Parallel computation of 3-D soil-structure interaction in time domain with a coupled FEM/SBFEM approach. *Journal of Scientific Computing*, 52, pp. 446–467.
Song, Ch. and Bazyar, M. H. (2008), Development of a fundamental-solution-less boundary element method for exterior wave problems. *Communications in Numerical Methods in Engineering*, 24, pp. 257–279.
Bazyar, M. H. and Song, Ch. (2008), A continued-fraction-based high-order transmitting boundary for wave propagation in unbounded domains of arbitrary geometry. *International Journal for Numerical Methods in Engineering*, 74, pp. 209–237.
Birk, C., Prempramote, S. and Song Ch. (2012), An improved continued-fraction-based high-order transmitting boundary for time-domain analyses in unbounded domains. *International Journal for Numerical Methods in Engineering*, 89, pp. 269–298.
Deeks, A. J. and Wolf, J. P. (2002), A virtual work derivation of the scaled boundary finite-element method for elastostatics. *Computational Mechanics*, 28, pp. 489–504.
Zienkiewicz, O. C., Taylor, R. L. and Zhu, J. Z. (2005), *The finite element method: its basis and fundamentals (Sixth edition)*. Elsevier Butterworth-Heinemann: Oxford.
Golub, G. H. and Van Loan, C. F. (1996), *Matrix Computations (Third edition)*. North Oxford Academic: Oxford.
Adhikari, S. and Wagner, N. (2004), Direct time-domain integration method for exponentially damped linear systems. *Computers and Structures*, 82, pp. 2453–2461.
Trinks, C. (2004), Consistent absorbing boundaries for time-domain interaction analyses using the fractional calculus. PhD Thesis, Dresden University of Technology: Dresden.
ABAQUS Inc. (2010), *ABAQUS Theory Manual, Version 6.10*. Providence, RI, USA.